International Journal of Mechanical, Industrial and Aerospace Sciences
ISSN: 2517-9950
Vol:6, No:5, 2012

Effects of Mold Surface Roughness on Compressible Flow of Micro-Injection Molding

Nguyen Q. M. P., Chen X., Lam Y. C., Yue C. Y.

Abstract**—**Polymer melt compressibility and mold surface roughness, which are generally ignored during the filling stage of the conventional injection molding, may become increasingly significant in micro injection molding where the parts become smaller. By employing the 2.5D generalized Hele-Shaw model, we presented here the effects of polymer compressibility and mold surface roughness on mold-filling in a micro-thickness cavity. To elucidate the effects of surface roughness, numerical investigations were conducted using a cavity flat plate which has two halves with different surface roughness. This allows the comparison of flow field on two different halves under identical processing conditions but with different roughness. Results show that polymer compressibility and mold surface roughness have effects on mold filling in micro injection molding. There is in shrinkage reduction as the density is increased due to polymer melt compressibility during the filling stage.

Keywords**—**Compressible flow; Micro-injection molding, Polymer; Surface roughness

I. Introduction

MICRO-injection molding is one of the key manufacturing processes for mass production of micro-parts due to its many advantages such as low cost, short cycle times, full automation capabilities, accurate replication and dimensional control, etc. The injection molding cycle typically consists of three phases, namely filling, post-filling and cooling phases. Although the know-how of macro scale injection molding can generally be transferable to micro injection molding, there are significant and important differences between these two processes. Indeed, melt flow behavior in a micro cavity is not yet sufficiently understood.

Existing simulation software for macro injection molding can predict the flow field in conventional macro injection molding rather successfully. However, they might not work well for micro injection molding for the whole range of processing conditions. The discrepancies between simulation and experimental results for the micro scale may be due to (a) the neglect of melt compressibility during mold filling, (b) the neglect of micro-scaled factors such as surface roughness, wall slip, etc. and (c) the lack of good quality material databases for simulation. Polymer compressibility affects both the pressure distributions and the part density. As relatively high injection pressure is recommended for micro-injection molding to prevent short shots, the compressibility of polymer melt should be considered as it could have an effect on shrinkage and warpage.

Nguyen Q. M. P. is with the Singapore-MIT Alliance, Manufacturing Systems & Technology Programme, Ph.D student, Nanyang Technological University, 637460, Singapore (e-mail: nguy0098@e.ntu.edu.sg).

Chen X. is with the Singapore-MIT Alliance, Manufacturing Systems & Technology Programme, Research Fellow, Nanyang Technological University, 637460, Singapore (e-mail: mxchen@ntu.edu.sg).

Lam Y. C. is with the Singapore-MIT Alliance, Manufacturing Systems & Technology Programme, Professor in the School of Mechanical and Aerospace Engineering, Nanyang Technological University, 639798, Singapore (e-mail : myclam@ntu.edu.sg).

Yue C. Y. is with the Singapore-MIT Alliance, Manufacturing Systems & Technology Programme, Professor in the School of Mechanical and Aerospace Engineering, Nanyang Technological University, 639798, Singapore (e-mail: mcyyue@ntu.edu.sg).

Surface roughness is generally ignored in injection molding of macro-parts. However, as the cavity dimensions decrease in micro-parts, surface roughness could become significant relative to the other dimensions of the mold and thus could not be ignored. Recently, this research group [1-5] investigated numerically and experimentally the effects of surface roughness on mold filling into micro-disked part and had obtained good agreement between experimental and simulated results. However, the combined effects of mold surface roughness and melt compressibility are yet to be addressed.

By developing our in-house code which adopts the 2.5D Hele-Shaw approximation and takes into considerations the melt compressibility and surface roughness, we elucidate experimentally and numerically the effects of polymer compressibility and mold surface roughness on the filling of micro-thickness cavity.

II. Modelling

In this study, we follow the method of Hieber and Shen [6] and Chiang et al [7-8]. The modified generalized Hele-Shaw model which incorporates the polymer melt compressibility and surface roughness was obtained. A hybrid FEM/ FDM approach was employed to calculate the pressure/ temperature field and the melt front was captured using the control volume method. The rheological behavior of the polymer melt was modeled using the widely accepted Cross-WLF model, while the compressible behavior was assumed to obey the two domain Tait equation of state. Details of the numerical implementation can be found in our previous paper [9].

Following Ong et al [5], we employed the three dimensional average roughness S_a, which can be measured easily using 3D surface profilometer, as the parameter to characterize the surface roughness. The equivalent three-dimensional homogeneous pyramid roughness profile (see Fig. 1) was used to represent the physical surface roughness of the mold cavity. The effective roughness height (δ) in terms of the average surface roughness is $\delta=3S_a$. Thus, the volume fraction Φ can be obtained as [5]

$$\Phi=\begin{cases}1-\frac{1}{2}\left(1-\frac{y}{\delta}\right)^2 & 0\le y\le\delta\\ \frac{1}{2}\left(1+\frac{y}{\delta}\right)^2 & -\delta\le y<0\end{cases} \quad (1)$$

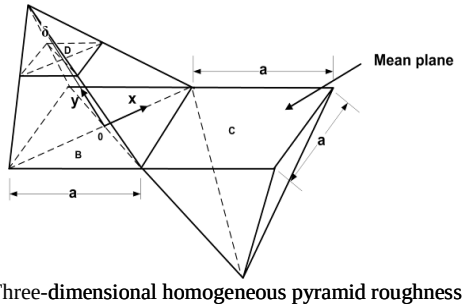

Fig. 1 Three-dimensional homogeneous pyramid roughness profile [5]

The shrinkage index can be calculated as the difference between the part density at melting temperature at the end of filling and that at room temperature, which is:

$$\text{shrinkage index} = \frac{\rho_0 - \rho}{\rho_0} \times 100\% \quad (2)$$

where ρ and ρ_0 is the density at temperature at the end of filling and that at room temperature (25°C) respectively.

The effect of surface roughness on heat transfer is modeled as a homogenous roughness layer characterized by its effective (equivalent) density, thermal conductivity, heat capacity and effective height δ.

Based on a simple rule of mixture, the effective density within the roughness layer may be written as:

$$\rho = \rho_1(1-\Phi) + \rho_2\Phi \quad (3)$$

where ρ_1 and ρ_2 are the density of the melt and the mold respectively. Similarly, the effective specific heat of the roughness layer is written as:

$$C_p = C_{p1}(1-\Phi) + C_{p2}\Phi \quad (4)$$

where C_{p1} and C_{p2} are the specific heat of the melt and the mold respectively.

To estimate the effective thermal conductivity k of the roughness layer, Jeffrey's equation is adopted, which provides a better approximation than the linear rule of mixture. The Jeffrey's equation can be represented as [10]

$$k = \left\{1 + 3\zeta\Phi + \Phi^2(3\zeta^2 + \frac{3\zeta^3}{4} + \frac{9\zeta^3}{16}\frac{\lambda+2}{2\lambda+3} + \frac{3\zeta^4}{64})\right\} \cdot k_1 \quad (5)$$

where $\lambda = k_2/k_1$ and $\zeta = (\lambda-1)/(\lambda+2)$, with k_1 and k_2 the thermal conductivity of the polymer melt and mold respectively.

III. Experiment

The experiments were conducted using a 25 ton injection molding machine Battenfeld HM 25/60. A micro thickness rectangular cavity, which is 40mm long, 24mm wide and 420μm thick, was chosen to demonstrate the effects of polymer melt compressibility and mold surface roughness during mold filling. A two plate mold was fabricated to produce the designed plastic part. The polymer melt was injected into the mold cavity through the pin gate. To measure the cavity pressure and mold wall temperature during the filling phase, one pressure-temperature sensor of ϕ4mm (Kistler Type 6190CA) was installed near the gate as shown in Fig.2. A data acquisition system (Kistler CoMo-Injection) was employed for logging the pressure and temperature data.

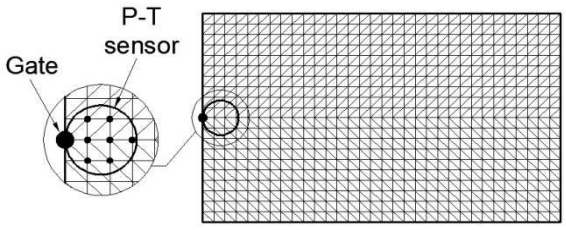

Fig. 2 Mesh for cavity [9]

IV. Results And Discussion

The material used in this investigation was high flow COC TOPAS 5013L-10 produced by TOPAS Advanced Polymers. Its properties, such as physical properties, PVT data and especially pressure-dependent viscosity were tested and provided by Autodesk Australia Pty. Ltd.

The melt density, glass transition temperature, specific heat and thermal conductivity of TOPAS 5013L-10 are 904kg/m^3, 125°C, 2777.667 J/kg.K and 0.194 W/m.K respectively.

The Cross-WLF model may be written as:

$$\eta = \frac{\eta_0(T,p)}{1 + (\eta_0\dot{\gamma}/\tau^*)^{1-n}} \quad (6)$$

$$\eta_0(T,p) = D_1 \exp\left\{-\frac{A_1[T - T^*(p)]}{A_2 + [T - T^*(p)]}\right\} \quad (7)$$

where

$$T^*(p) = D_2 + D_3 p \quad (8)$$

$$A_2(p) = \tilde{A}_2 + D_3 p \quad (9)$$

The seven constants for the model, i.e n, τ^*, D_1, D_2, D_3, A_1 and $\tilde{A}_2$ are contained in table I.

The two domain Tait equation of state for amorphous material may be written as:

$$v(T,p) = v_0(T)\left[1 - C\ln\left(1 + \frac{p}{B(T)}\right)\right] \quad (10)$$

where the material constant $C = 0.0894$. $v_0(T)$ and $B(T)$ are denoted by

$$v_0(T) = \begin{cases} b_{1,l} + b_{2,l}(T - b_5) & if \quad T \geq T_t(p) \\ b_{1,s} + b_{2,s}(T - b_5) & if \quad T < T_t(p) \end{cases} \quad (11)$$

$$B(T) = \begin{cases} b_{3,l}\exp[-b_{4,l}(T - b_5)] if & T \geq T_t(p) \\ b_{3,s}\exp[-b_{4,s}(T - b_5)] if & T < T_t(p) \end{cases} \quad (12)$$

$$T_t(p) = b_5 + b_6 p \quad (13)$$

where T_t is the pressure-dependent glass transition temperature for an amorphous polymer. $b_{1,l}$, $b_{2,l}$, $b_{3,l}$, $b_{4,l}$, $b_{1,s}$, $b_{2,s}$, $b_{3,s}$, $b_{4,s}$, b_5 and b_6 are material constants which are contained in table II.

The density, specific heat and thermal conductivity of the mold steel material are 7820 kg/m^3, 500 J/kg.K and 32 W/m.K respectively. The mold temperature (46°C), melt temperature (300°C), injection speed (200 mm/s) and cooling times (15s) were set for the injection molding experiments. To obtain consistent plastic parts, the specimens of five consecutive runs were collected only after ten cycles of the injection process.

TABLE I
Cross-WLF constants for TOPAS 5013L-10

Symbol	Quantity
n	0.40271
τ^* (Pa)	46129.8
D_1 (Pa.s)	4.51108e+017
D_2 (K)	343.15
D_3 (K/Pa)	1.200E-7
A_1	44.743
$\tilde{A}_2$ (K)	51.6

TABLE II
TAIT PVT CONSTANTS FOR TOPAS 5013L-10

Symbol	Quantity
$b_{1,l}$ (m^3/kg)	0.001012
$b_{2,l}$(m^3/kg.K)	6.693000E-07
$b_{3,l}$(Pa)	1.690210E+08
$b_{4,l}$(1/K)	0.004276
$b_{1,s}$(m^3/kg)	0.001012
$b_{2,s}$ (m^3/kg.K)	2.310000E-07
$b_{3,s}$ (Pa)	2.805470E+08
$b_{4,s}$ (1/K)	0.002380
b_5 (K)	402.55
b_6 (K/Pa)	4.694000E-07

The finite element mesh used in this simulation is shown in Fig. 2 (1280 elements, 693 nodes). The filling time was 0.18s. Fig. 3 shows the schematic diagram of mold cavity for the simulation of *compressible flow* used in this study. The effective roughness height (δ) on the smooth half (upper half) was set to be 0 μm and 40μm on the rough half (lower half) (see Fig. 3b). It should be noted that for simplicity, a smooth roughness of 0μm for both halves of the mold was used to verify the effect of compressibility (see Fig. 3a).

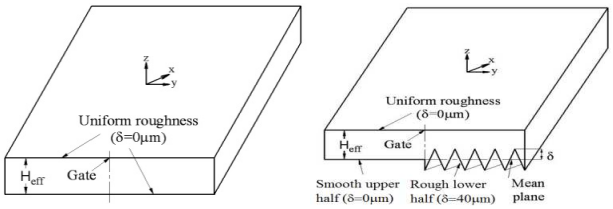

(a) (b)

Fig. 3 Schematic diagram of mold cavity for simulation of compressible flow. (a) without and (b) with mold surface roughness effect. Note: diagram rotated 90 degree with respect to the physical orientation of the mold

Figure 4 shows the cavity pressure during the filling stage of three measured pressure traces with that of the simulated incompressible and compressible flows without surface roughness effect, i.e. when all surfaces of the mold were smooth (note: experimentally measured "smooth" surface roughness was S_a=0.23μm, and for simplicity was assumed to have zero roughness in the simulations). Here 'incompressible ' and 'compressible ' flows refer to the simulated filling flow without and with compressibility effects. Figure 4 indicates that that there is little pressure difference between non-compressibility and compressibility flows at low pressure during the initial filling stage. However, with the advancement of filling, the simulated pressure for compressible flow fits the experimental results better than that of incompressible flow. Thus, compressibility effects should not be ignored in flow simulation for thin cavity.

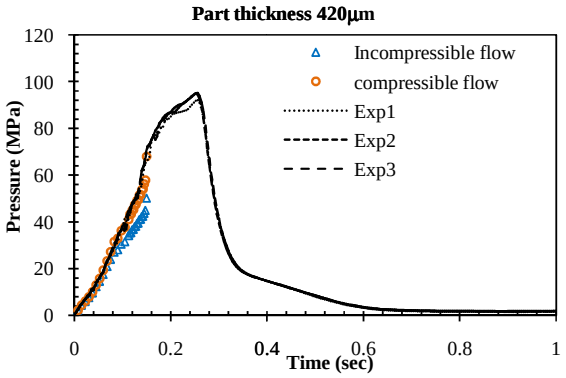

Fig. 4 Comparison of cavity pressure between experiments (curves) and simulations with and without melt compressibility effect (symbols) for part thickness of 420μm and without surface roughness

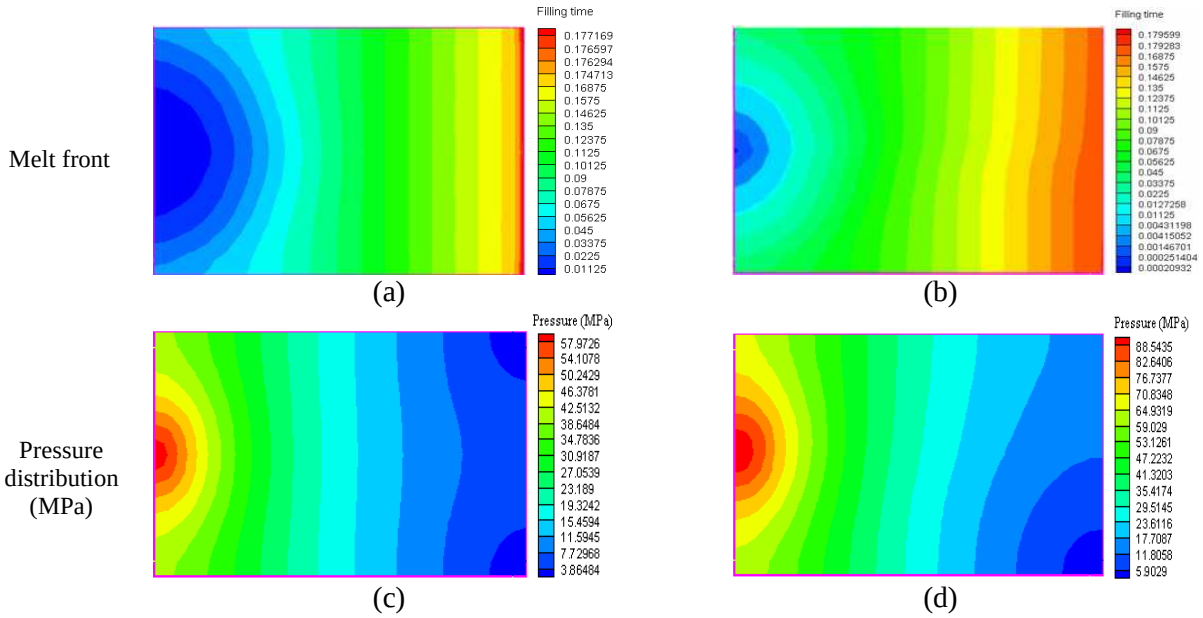

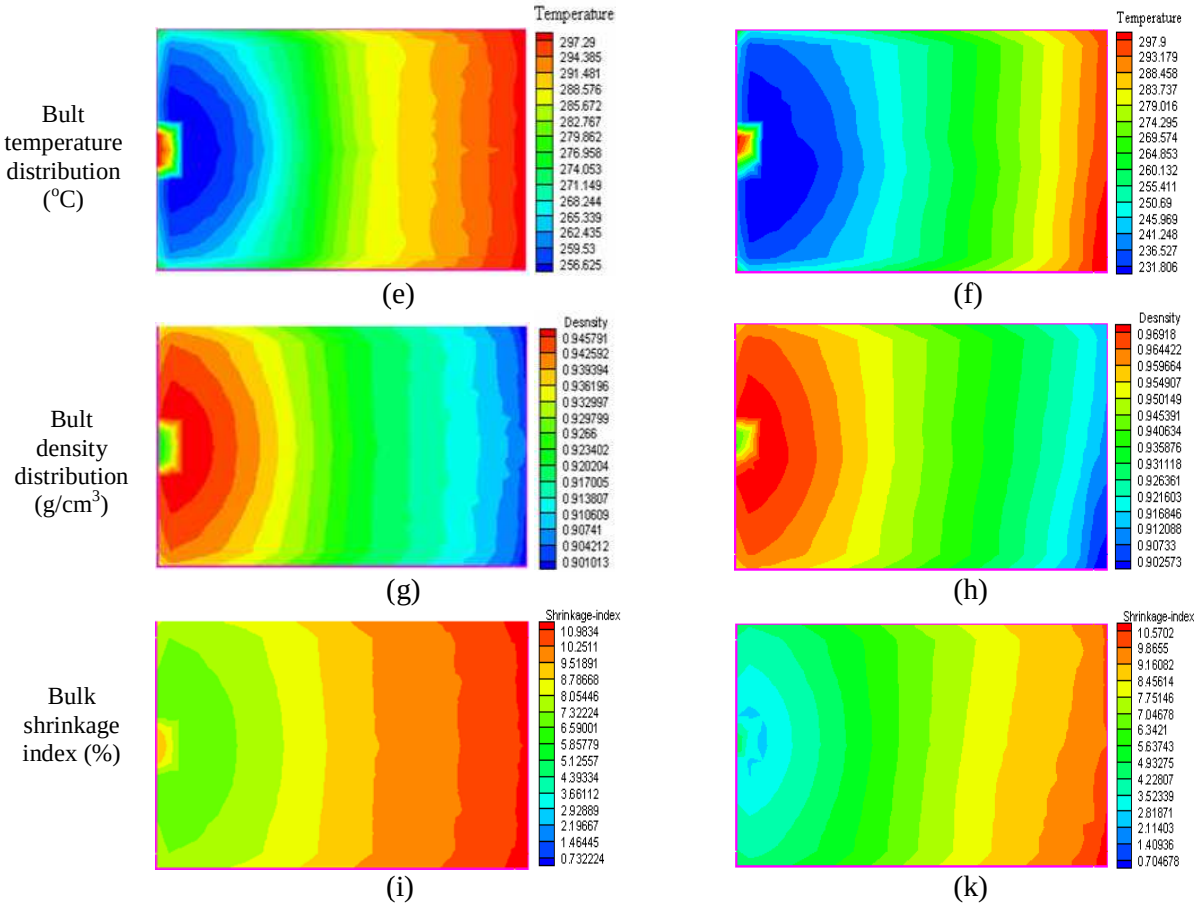

Fig. 5 Bulk distribution inside cavity with melt compressibility effect -- (a,c,e,g,i) without surface roughness, i.e. $\delta_{upper}=\delta_{bottom}=0\mu m$ at both the upper and bottom halves and (b,d,f,h,k) with surface roughness, i.e. $\delta_{bottom}=40\mu m$ at the bottom half and $\delta_{upper}=0\mu m$ at the upper half

Fig. 5 presents the predicted melt flow front, pressure, bulk temperature, density and shrinkage index distribution inside the mold cavity for *compressible flow*. Fig. 5a, 5c, 5e, 5g, 5i are for flow without mold surface roughness effect (i.e. 0μm for both upper and lower halves – see Fig. 3a), and Fig. 5b, 5d, 5f, 5h, 5k are for flow with mold surface roughness effect (i.e. 40μm at the lower half and 0μm at the upper half for the lower surface of the mold- see. Fig. 3b). As shown in Fig. 5a, the melt flow front is symmetrical and gradually flatten away from the gate, whereas in Fig. 5b, the rougher surface at the lower half (δ=40μm) hinders the flow and a non-uniform flow front is obtained as expected. With a constant injection rate, the shear rates will increase with a decrease of effective thickness due to roughness. As polymer melt exhibits shear thinning behavior, a higher shear rate will reduce melt viscosity, which will enhance fluidity. In addition, with shear heating being more pronounced for the thinner section due to roughness, the melt temperature will increase. This will reduce viscosity further. However, the polymer melt tends to freeze more quickly due to the enhancement of heat loss through the mold wall due to mold roughness. This will decrease the melt temperature and increase its viscosity. Thus, the effect of roughness is rather complicated. However, in general, the increase of viscosity due to a lowering of temperature as a result of more heat loss through the rougher half will be more dominant. In addition, a higher pressure gradient will be required to achieve the same volume flow rate for a thinner section with mold roughness. As shown in Fig. 5, this required high injection pressure for the thinner section will result in more compressibility, higher packing density and lower shrinkage index. This agrees well with Theilade's experimental finding [11], i.e. a rougher surface will yield a lower shrinkage of polymer due to a higher packing density.

V. Conclusions

We have presented here the effects of polymer melt compressibility and mold surface roughness on mold-filling of micro-thickness cavities of 420 μm by using a generalized compressible Hele-Shaw model. To take into consideration the roughness effects in numerical investigation, the three-dimensional homogenous pyramid roughness model was employed.

Our numerical investigation indicates that surface roughness and compressibility of the melt have effects on the melt flow front, cavity pressure, part density as well as part shrinkage. Additional experimental investigation on the effect of mold surface roughness on the compressible flow is currently underway to verify the validity of the numerical simulation.

ACKNOWLEDGMENT

The authors would like to acknowledge the research funding supported by the Singapore-MIT Alliance Program. Thanks are also extended to Autodesk Australia Pty. Ltd. for material characterization.

REFERENCES

[1] H. L. Zhang, N. S. Ong and Y. C. Lam 2007 Effects of surface roughness on microinjection molding Polymer Engineering and Science 47 2012-2019
[2] H. L. Zhang, N. S. Ong and Y. C. Lam 2008 Experimental investigation of key parameters on the effects of cavity surface roughness in microinjection molding Polymer Engineering and Science 48 490-495
[3] H. L. Zhang, N. S. Ong and Y. C. Lam 2008 Mold surface roughness effects on cavity filling of polymer melt in micro injection molding International Journal of Advanced Manufacturing Technology 37 1105-1112
[4] N. S. Ong, H. L. Zhang and Y. C. Lam 2008 Numerical simulation of cavity roughness effects on melt filling in microinjection molding Advances in Polymer Technology 27 89-97
[5] N. S. Ong, H. L. Zhang and Y. C. Lam 2009 Three-dimensional modeling of roughness effects on microthickness filling in injection mold cavity International Journal of Advanced Manufacturing Technology 1-9
[6] C. A. Hieber and S. F. Shen 1980 A finite-element/finite-difference simulation of the injection-molding filling process Journal of Non-Newtonian Fluid Mechanics 7 1-32
[7] H. H. Chiang 1991 A unified simulation of the filling and postfilling stages in injection molding, part 1: Formulation Polymer Engineering and Science 31 116-124
[8] H. H. Chiang, C. A. Hieber and K. K. Wang 1991 A unified simulation of the filling and postfilling stages in injection molding. Part ii: Experimental verification Polymer Engineering & Science 31 125-139
[9] Q. M. P. Nguyen, X. Chen, Y. C. Lam and C. Y. Yue 2011 Effects of polymer melt compressibility on mold filling in micro-injection molding Journal of Micromechanics and Microengineering 21
[10] Y. C. Lam, X. Chen, K. C. Tam and S. C. M. Yu 2003 Simulation of particle migration of powder-resin system in injection molding Journal of Manufacturing Science and Engineering 125 538-547
[11] U. R. A. Theilade, E. Kjœr and H. N. Hansen The effect of mold surface topography on plastic part in-process shrinkage in injection molding 2003 Nashville, TN